Semi-mechanistic modeling of resistance development to β-lactam and β-lactamase-inhibitor combinations

Tandar, S.T.; Aulin, L.B.S.; Leemkuil, E. M.J.; Liakopoulos, A.; Hasselt J.G.C. van

Journal of Pharmacokinetics and Pharmacodynamics (2024) 51:199–211
https://doi.org/10.1007/s10928-023-09895-3

ORIGINAL PAPER

Semi-mechanistic modeling of resistance development to β-lactam and β-lactamase-inhibitor combinations

Sebastian T. Tandar[1] · Linda B.S. Aulin[1,2] · Eva M. J. Leemkuil[1] · Apostolos Liakopoulos[1,3] · J. G. Coen van Hasselt[1]

Received: 16 May 2023 / Accepted: 27 October 2023 / Published online: 26 November 2023

Abstract

The use of β-lactam (BL) and β-lactamase inhibitor (BLI) combinations, such as piperacillin-tazobactam (PIP-TAZ) is an effective strategy to combat infections by extended-spectrum β-lactamase-producing bacteria. However, in Gram-negative bacteria, resistance (both mutational and adaptive) to BL-BLI combination can still develop through multiple mechanisms. These mechanisms may include increased β-lactamase activity, reduced drug influx, and increased drug efflux. Understanding the relative contribution of these mechanisms during resistance development helps identify the most impactful mechanism to target in designing a treatment to counter BL-BLI resistance. This study used semi-mechanistic mathematical modeling in combination with antibiotic sensitivity assays to assess the potential impact of different resistance mechanisms during the development of PIP-TAZ resistance in a *Klebsiella pneumoniae* isolate expressing CTX-M-15 and SHV-1 β-lactamases. The mathematical models were used to evaluate the potential impact of several cellular changes as a sole mediator of PIP-TAZ resistance. Our semi-mechanistic model identified 2 out of the 13 inspected mechanisms as key resistance mechanisms that may independently support the observed magnitude of PIP-TAZ resistance, namely porin loss and efflux pump up-regulation. Simulation using the resulting models also suggested the possible adjustment of PIP-TAZ dose outside its commonly used 8:1 dosing ratio. The current study demonstrated how theory-based mechanistic models informed by experimental data can be used to support hypothesis generation regarding potential resistance mechanisms, which may guide subsequent experimental studies.

Keywords Piperacillin-Tazobactam · Antimicrobial resistance · *Klebsiella pneumoniae* · Semi-mechanistic model

Introduction

Antimicrobial resistance in Gram-negative bacteria poses a major threat to public health [1]. One of the concerns is associated with the expression of extended-spectrum β-lactamases (ESBLs), which confers antibiotic resistance to β-lactams (BLs) [2], a cornerstone antibiotic class to treat Gram-negative infections. BL-type antibiotics exert its bactericidal effect by inhibiting the activity of penicillin binding proteins (PBP) in the periplasm. One treatment strategy against ESBL-producing strains is the co-administration of β-lactamase inhibitors (BLIs) alongside BL-antibiotics [3]. BLIs lack bactericidal activity on their own but protect the co-administered BL antibiotic from degradation by β-lactamases [3, 4]. Piperacillin-tazobactam (PIP-TAZ) is a commonly used BL-BLI combination that is mainly prescribed for the treatment of Gram-negative bacterial infections [4].

Despite the success of the combination, resistance against PIP-TAZ has been reported [5, 6]. In this study, the term 'resistance' is used to generally describe the decrease in antibiotic sensitivity observed as changes on bacterial population growth rate without distinguishing the mutational or adaptive nature of its development. In Gram-negative bacteria, resistance to BL-BLI combination is mainly achieved through elevated β-lactamase activity [7], reduced drug influx through the outer membrane [8], or increased drug efflux [8, 9] (Fig. 1).

✉ Sebastian T. Tandar
s.t.tandar@lacdr.leidenuniv.nl

✉ J. G. Coen van Hasselt
coen.vanhasselt@lacdr.leidenuniv.nl

[1] Leiden Academic Centre for Drug Research, Leiden University, Leiden, The Netherlands

[2] Department Clinical Pharmacy and Biochemistry, Freie Universität Berlin, Berlin, Germany

[3] Department of Biology, Utrecht University, Utrecht, The Netherlands

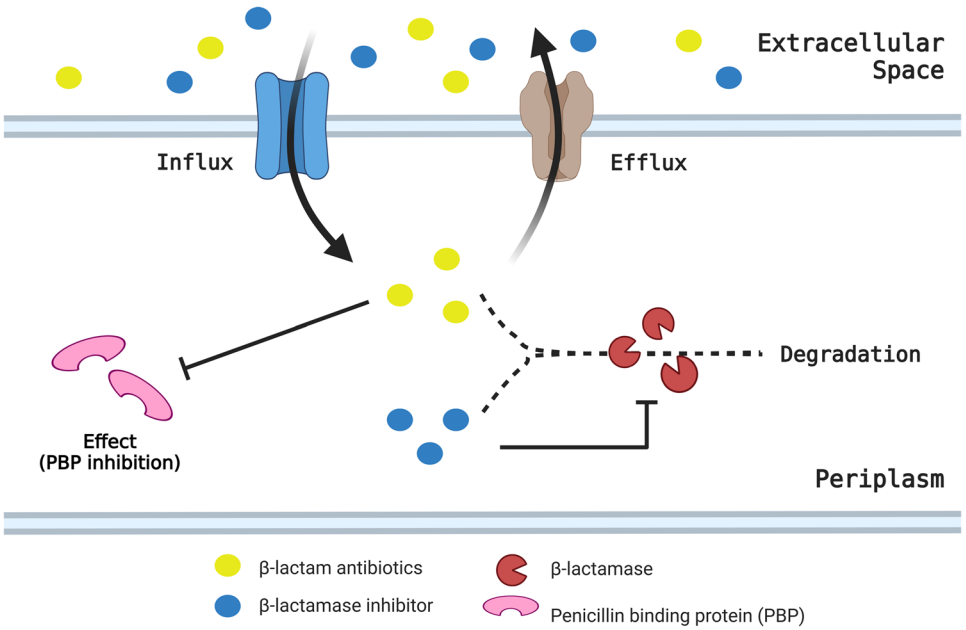

Fig. 1 PIP-TAZ transfer and bactericidal effect in the periplasmic space. Periplasmic (*pp*) accumulation of PIP and TAZ are determined by their influx, efflux, and degradation. Bactericidal effect through PBP inhibition was assumed to be a function of periplasmic PIP concentration and was empirically expressed using the Hill equation. Pointed arrows represented mass transfer through the outer membrane, dashed lines represent degradation, and blunt arrow represent inhibitory activity

These resistance mechanisms may decrease the effective BL concentration in the periplasm, thereby reducing the bactericidal effect exerted on the bacteria [10]. Although these mechanisms may simultaneously contribute to promoting PIP-TAZ resistance, assessing the potential importance of each individual mechanism may allow guide the rational design of treatments countering emergence of resistance.

Comprehensive quantitative assessment of the relative contribution of potential resistance mechanisms is a complex task. While the effect of a specific resistance mechanism can be targeted by experimental assays [11–13], conclusion drawn from such observations may be convoluted by the concurrence of multiple resistance mechanisms.

Unlike experimental assays, semi-mechanistic mathematical models representing the transfer and effect of antibiotics can be adjusted freely to highlight the effect of one (set of) cellular change towards antimicrobial resistance. This allows mathematical models to be used as a hypothesis-generating tool to identify key antibiotic resistance mechanism(s) based on prior knowledge [14, 15]. The primary objective of this study was to showcase the utility of semi-mechanistic models as a means of theoretical exploration to understand the potential impact of different cellular mechanisms that may mediate PIP-TAZ resistance, and subsequently help identify cellular mechanisms that may be prioritized in future studies. Additionally, we demonstrated how a semi-mechanistic may be used to as a supplementary tool to support the design of antibiotic treatment against resistance.

Methods

Bacterial strain and culture condition

The current study focused on *K. pneumoniae* isolate GR116.26, which harbored a genomic copy of $bla_{\text{CTX-M-15}}$ and $bla_{\text{SHV-1}}$ β-lactamase genes [16]. $bla_{\text{SHV-1}}$ β-lactamase was generally expected from most *K. pneumoniae* strains [16]. All liquid cultures were carried out in cation-adjusted Mueller-Hinton (MH) broth (Becton Dickinson) and were incubated at 37 °C.

Antibiotic sensitivity assays

Checkerboard assays were performed to approximate PIP and TAZ concentration ranges to be included in the main static time-kill (STK) assay. Checkerboard assays were carried out on a in 96-well plates (Greiner Bio-One, flat bottom, 200 µl culture scale with 200 rpm orbital shaking). The checkerboard assay included 66 PIP-TAZ concentration combinations with PIP and TAZ concentrations

ranging from 0 to 256 mg/L and 0 to 16 mg/L, respectively (Fig. S2). Bacterial growth was monitored by optical density at 600 nm (OD_{600}; BMG Fluostar Omega).

STK assays were performed to characterize the pharmacodynamics of PIP-TAZ combination. STK assays were carried out on a 20 mL scale with 150 rpm linear shaking. This assay included 17 PIP-TAZ concentrations ranging from 0 to 16 mg/L and 0 to 256 mg/L for PIP and TAZ, respectively. These concentrations were selected based on the result of the preceding checkerboard assay. STK cultures were sampled (500 µL) at 0, 1, 2, 3, 4, 5, 6, 7, 24, and 48 h after the inoculation, giving an end volume of approximately 15 mL. Serial dilutions (10-fold dilution at each dilution steps) were performed using 0.9% (w/v) drug-free NaCl solution to achieve a final colony count of 20–200 colonies on the agar plate. Undiluted samples were also plated when low cell density was expected. The samples were not subjected to antibiotic removal (cell washing) prior to dilution and/or plating to mitigate potential cell loss, particularly in samples with low cell density. Consequently, there may have been antibiotic carryover in less diluted samples. 50 µL of the resulting (un)diluted sample on drug-free MH agar plates (VWR™ MH and APC Pure bacteriological agar) using Whitley Automatic Spiral Plater with Vacuum Source 602 for colony forming units (CFU) measurement (400 CFU/mL lower limit of quantification; LLOQ).

Both assays were performed with a starting inoculum of approximately 10^6 CFU/mL. Drugs were added to the culture medium before inoculation. Assays were performed in triplicates.

Model structure

PIP-TAZ mass transfer

Porin-mediated import of PIP-TAZ across the bacterial outer membrane was assumed to follow Fick's law of passive diffusion (Eq. 1) [10, 17]. Here, P and A represent membrane permeability and surface area, respectively. The transfer was assumed to be driven by concentration gradient between the external/assay drug concentration (C_{ext}) and the periplasmic drug concentration (C_{pp}). Porin was assumed to act as passive transport mediator. Porin expression is thus assumed to be linearly correlated to membrane permeability ($P \propto [porin]$)

$$\left(\frac{dC_{pp}}{dt}\right)_{import} = P \times A \times \left(C_{ext} - C_{pp}\right) \quad (1)$$

PIP-TAZ efflux by the efflux pumps were described using Michaelis-Menten equation adjusted for cooperativity [18] (Eq. 2). Here, PIP-TAZ efflux rate was expressed using $V_{efflux,\ max}$, K_{efflux}, and h, which represent the maximum rate of efflux, drug-efflux pump binding coefficient, and Hill exponent, respectively. Since the equation was derived from the Michaelis-Menten kinetics, $V_{efflux,\ max}$ was assumed to be proportional to efflux pump expression.

$$\left(\frac{dC_{pp}}{dt}\right)_{efflux} = -V_{efflux,max} \times \frac{C_{pp}^h}{C_{pp}^h + K_{efflux}^h} \quad (2)$$

Drug hydrolysis by β-lactamases was modeled using the Michaelis-Menten Eqs. [19, 20] (Eq. 3), where k_{cat}, $[Enzyme]$, and K_m represent the catalytic rate of the β-lactamases towards the substrate, enzyme concentration, and Michaelis constant of the β-lactamases towards the respective drug [19]

$$\left(\frac{dC_{pp}}{dt}\right)_{hydrolysis} = -k_{cat} \times [Enzyme] \times \frac{C_{pp}}{C_{pp} + K_m} \quad (3)$$

PIP-TAZ binding competition to β-lactamases and efflux pumps

The kinetics of PIP and TAZ binding to β-lactamases and efflux pumps were assumed to be competitive and reversible [19]. The effect of the competitive binding was reflected on the parameters K_{efflux} and K_m. Here, we assumed that only a single PIP or TAZ molecule can interact with one β-lactamase or efflux pump at a time. The effective value ($K_{effective}$) of these constants in the presence of the competitor at the periplasm ($C_{pp,competitor}$) is expressed by Eq. 4, where K represents the binding constant of the molecule of interest and $K_{competitor}$ represents the binding constant of the competitor molecule [19]

$$K_{effective} = K \times \left(1 + \frac{C_{pp,competitor}}{K_{competitor}}\right) \quad (4)$$

Periplasmic β-lactamase availability

The availability of CTX-M-15 and SHV-1 β-lactamases in the periplasm were described by its background expression level R_0 and its natural degradation rate k_{deg}. The value of k_{deg} was fixed to 0.01 (h^{-1}), as previously reported for most proteins in Gram-negative bacteria [21]. Additionally, TAZ degradation was assumed to inactivate the associated β-lactamase (suicide inhibition) [22]

$$\frac{d[Enzyme]}{dt} = R_0 \times k_{deg} - [Enzyme] \times k_{deg} + \left(\frac{dC_{TAZ,pp}}{dt}\right)_{hydrolysis} \quad (5)$$

Equation 5 infers that in the absence of TAZ, Image will be reached at the steady state. In the current study, the units of R_0 were kept as arbitrary unit to account for the differences in enzyme concentrations used in the assays reported in the reference studies [19, 20]. Absolute values of β-lactamase concentrations can be derived by multiplying the simulated enzyme units with the concentration of β-lactamase used in the referenced experiments for the specific β-lactamase.

Bacterial growth and bactericidal effect

The growth of a bacterial population (N) was described using the population-limited growth model with system carrying capacity of N_{max}. The effective (observed) growth rate of the bacterial population was assumed to be the sum of its natural growth rate (k_{growth}) and the effective kill rate (bactericidal effect) from being exposed to antibiotics (Eq. 6)

$$\frac{dN}{dt} = k_{growth} \times N \times \left(1 - \frac{N}{N_{max}}\right) - E \times N \quad (6)$$

The bactericidal effect exerted on the population as effective kill rate was represented as a function of the periplasmic concentration of bactericidal agent (PIP), i.e., $E = f(C_{pp})$. A Hill equation was selected as an empirical description for PIP bactericidal effect on the bacterial growth (Eq. 7), where E_{max}, $EC50$, and H represent respectively the maximum bactericidal effect, the PIP concentration required to achieve half-maximum kill rate, and the Hill exponent. The bactericidal effect of TAZ was negligible (Fig. S2) [4]

$$E = E_{max} \times \frac{C_{pp}^{H}}{C_{pp}^{H} + EC_{50}^{H}} \quad (7)$$

The development of resistance

The initial PIP-TAZ pharmacodynamics (before the point of regrowth) was described using a one-population model. (Fig. S1a) In a one-population model, the bacterial population was assumed to consist of only a single population which shared the same growth and drug sensitivity characteristics.

The STK assays allow merely phenotypic observation of resistance development (regrowth). Semi-mechanistic models were used to derive mechanistic understanding from such phenotypic observation. Here, a two-population growth model [23] was used to describe the resistance development (Fig. S1b). This model assumed the presence of a susceptible (N_S) and a resistant (N_R) bacterial population. The bacterial population was assumed to be fully susceptible at the start of the experiment. A first-order transfer rate ($k_{transfer}$) was used to empirically describe the transition of susceptible cells (N_S) into resistant cells (N_R). The drug effect exerted on the susceptible and resistant bacterial population was denoted by E_S and E_R, respectively. In the two-population growth models, the effective growth rates of both populations were determined by the sum of its growth, bactericidal effect that it experienced, and its susceptible-to-resistance transition (Eqs. 8 and 9)

$$\frac{dN_S}{dt} = k_{growth} \times N_S \times \left(1 - \frac{N_S + N_R}{N_{max}}\right) - E_S \times N_S - k_{transfer} \times N_S \quad (8)$$

$$\frac{dN_R}{dt} = k_{growth} \times N_R \times \left(1 - \frac{N_S + N_R}{N_{max}}\right) - E_R \times N_R + k_{transfer} \times N_S \quad (9)$$

In each model, the resistant population was assumed to possess a single mechanism of resistance. This resistance mechanism was depicted in the model as changes in one of its resistance-associated parameters (Eq. 10). Here, the value of a specific resistance-associated parameter was in the resistant population ($Parameter_{resistant}$) was assumed to be higher/lower to that of the susceptible population ($Parameter_{susceptible}$) with a factor of α. These resistance-associated parameters represented one of 13 parameters including outer membrane permeability, maximum efflux rate, efflux pump binding constant, β-lactamase expression level (CTX-M-15 and SHV-1), CTX-M-15 catalytic rate and Michaelis constant for PIP and TAZ, and SHV-1 catalytic rate and Michaelis constant for PIP and TAZ.

$$Parameter_{resistant} = \alpha \times Parameter_{susceptible} \quad (10)$$

Source of model parameters

Experimentally determined kinetic PIP-TAZ parameters were fixed to reported values (Table 1). Parameters related to strain growth (k_{growth}, N_{max}, inoculum size), drug effect ($Emax$, EC_{50}, H), and resistance development ($k_{transfer}$, α) were empirically fitted to experimental observations. At the time of the study, TAZ influx and efflux parameters were not available. The values of TAZ influx and efflux parameters were thus fixed to that of PIP. This decision was justified based on the knowledge that the permeability coefficient and maximum efflux rate across eight different β-lactams showed variation only within the same order of magnitude [18] (Table. S2). The assumptions made during the model development process are summarized on the supplementary Table S1.

Model parameter fitting

Mixed-effect model development and simulation were performed using 'nlmixr2' (v.2.0.7) and 'rxode2' (v.2.0.7)

Table 1 Literature-derived periplasmic transport parameters for PIP and TAZ

Parameters	Value	Units	References
PIP outer membrane permeability coefficient (P_{PIP})	3.67×10^{-5}	cm/s	[18] (mean)
Cell surface area (A)	132	cm^2/mg-cell	[18]
CTX-M-15 specific PIP hydrolysis rate ($k_{Cat,\ PIP,\ CTX-M-15}$)*	58	s^{-1}	[19]
CTX-M-15 Michaelis constant to PIP ($K_{m,\ PIP,\ CTX-M-15}$)*	32	µM	[19]
CTX-M-15 specific TAZ hydrolysis rate ($k_{Cat,\ TAZ,\ CTX-M-15}$)*	5.70×10^{-3}	s^{-1}	[19]
CTX-M-15 Michaelis constant to TAZ ($K_{m,\ TAZ,\ CTX-M-15}$)*	1.70×10^{-2}	µM	[19]
SHV-1 specific PIP hydrolysis rate ($k_{Cat,\ PIP,\ SHV-1}$)	86	s^{-1}	[20]
SHV-1 Michaelis constant to PIP ($K_{m,\ PIP,\ SHV-1}$)	91	µM	[20]
SHV-1 specific TAZ hydrolysis rate ($k_{Cat,\ TAZ,\ SHV-1}$)	0.1	s^{-1}	[20]
SHV-1 Michaelis constant to TAZ ($K_{m,\ TAZ,\ SHV-1}$)	7.00×10^{-2}	µM	[20]
PIP maximum efflux rate ($V_{efflux,\ max,\ piperacillin}$)	3.77×10^{-1}	nmol mg-cell^{-1} s^{-1}	[18]
PIP concentration for half-maximum efflux ($K_{efflux,\ PIP}$)	1.07	µM	[18]
PIP efflux Hill coefficient (h)	3.97		[18]
Protein (β-lactam) turnover rate ($k_{degradation}$)	0.01	h^{-1}	[21]

Parameters were measured in or with protein derived from *Escherichia coli*, except for those marked with (*), which were derived from *Enterobacter cloacae*-derived CTX-M-15 β-lactamase

packages in R (v.4.2.1). Mixed-effect models included a random effect term on inoculum size to account for possible variability related to the inoculation step. Initial estimates for model fitting routines were determined using particle swarm optimization (PSO; 'pso' package; v.1.0.3). Parameter fitting was performed based on STK assay observation. CFU measurements with values below the LLOQ (400 CFU/mL) were replaced with LLOQ/2.

Model parameters were fitted sequentially to prevent identifiability issues. The values for k_{growth} and N_{max} were estimated based on observation from the no-drug control and were fixed in subsequent model fitting steps. Drug effect parameters were fitted from observation made in the first 5 h of the experiment using the one-population model and were fixed in two-population models. Parameters related to resistance were fitted using the full 48-hours observation data.

Resistance mechanism evaluation

Two-population models (Fig. S1b) were used to assess the extent of cellular changes (α, Eq. 10) required for a specific resistance mechanism to describe the observed regrowth in our STK experiment. Here, PIP-TAZ resistance in the resistant sub-population was depicted as a change in one of the 13 resistance mechanism-associated parameters. Resistance mechanisms were thus individually represented in 13 semi-mechanistic models. By fitting the models to experimental observations, we estimated the extent of cellular changes (represented as α on Eq. 10) required by the initial susceptible population to show the observed level of resistance. The physiological feasibility of each resistance mechanism was then evaluated by comparing the extent of cellular changes estimated by our model to the extent of cellular changes reported for a resistant strain with respect to a susceptible strain of reference.

Growth inhibition simulation

Model simulations were performed to explore how specific resistance mechanisms may influence the survivability of the strain in different PIP-TAZ concentrations. The current simulation was also used to evaluate the potential of PIP-TAZ dose adjustment to counter a specific resistance mechanism. This analysis was performed using the porin down-regulation and efflux pump up-regulation. Simulation was performed using a starting inoculum size of 10^5 CFU/mL and included PIP-TAZ concentration ranges of 1 to 512 mg/L and 0.125 to 512 mg/L for PIP and TAZ, respectively. Each PIP-TAZ concentration combination was evaluated based on the bacterial density at the 24th hour of the culture predicted by the three models. For this analysis, we considered bacterial growth to be suppressed if the simulated cell density at the 24th hour was less than the inoculum size.

Parameter sensitivity analysis

Parameter sensitivity analysis was performed to investigate the impact of deviations in literature-based parameters. The sensitivity analysis focused on four selected PIP-TAZ concentrations, specifically 0–0, 4 – 2, 16 – 4, and 256 – 16 mg/L PIP-TAZ, to cover concentrations where different magnitudes of initial bactericidal effects were

observed. Absolute sensitivity coefficients ($S_{absolute}$) were derived from the absolute value of the ratio of the shift in total bacterial load (L; the area under the bacterial growth curve) relative to the shift in the value of a specific parameter of interest, denoted by β (Eq. 11). The ratios of parameter shift investigated in the analysis ranged from 0.25 to 1.75, with increments of 0.25

$$S_{absolute} = \frac{L/L_{original}}{\beta/\beta_{original}} \quad (11)$$

Results

Preliminary description of PIP-TAZ pharmacodynamics to *K. pneumoniae* GR116.26

Our study used STK assays to investigate the behavior of a CTX-M-15-producing *K. pneumoniae* strain in different concentrations of PIP-TAZ. From this experiment, we could see how the presence of both PIP and TAZ was required to achieve an initial population decline. In the presence of both PIP and TAZ, increasing PIP and/or TAZ concentrations resulted in a higher bactericidal effect as seen by the initial population decline observed at higher PIP-TAZ concentrations (Fig. S3). Even though an initial population decline was observed in some PIP-TAZ concentrations, in most cases, the population was able to regrow at approximately 5 h after inoculation (Fig. S3; grey lines). Given the timeframe of the observed regrowth and the stability of PIP and TAZ over 24 h [24, 25], it was likely that the observed regrowth was due to the development of resistance – as indicated as apparent decrease in observed PIP-TAZ bactericidal activity.

One-population model was used to describe the behavior of the strain in different PIP-TAZ concentrations before the onset of regrowth (Table 2, Fig. S4). This initial model demonstrated the impact of TAZ on the concentration-effect curve of PIP-TAZ (Fig. 2; Fig. S5). As illustrated in Fig. 2, an increase in TAZ concentration could achieve a bactericidal effect equal to the natural growth rate of the strain (indicated by the red dashed line) with a lower concentration of PIP. Additionally, this model can be used to simulate how changes in a specific resistance mechanism may impact the effect of PIP-TAZ on bacterial growth. Here, we simulated how changes in the values of 13 resistance mechanism-associated parameter may impact effective antibiotic kill rate at 16 – 4 mg/L PIP-TAZ concentration (Fig. 2b).

Model-based assessment of resistance mechanisms

The following analysis aimed to predict and assess the magnitude of changes required to convey resistance to the observed PIP-TAZ concentrations. The current analysis included 13 models, each depicting one of the thirteen potential mechanisms evaluated in the current study (Fig. 2b). Our models predicted the extent of cellular changes required for the strain to achieve the observed level of PIP-TAZ resistance (Fig. 3; Table 3; associated $k_{transfer}$ values for each resistance models summarized on Fig. S6).

The obtained model estimates were compared with literature reports to assess the physiological feasibility of each mechanism to serve as a single mediator of PIP-TAZ resistance. This was then followed by the selection of resistance mechanisms that required changes that were less extreme than that reported in the literature (Table 3). Based on this analysis, 8 out of the 13 resistance mechanisms were predicted to require cellular changes that were more extreme than what was previously reported for the mechanism. For example, our model predicted that an 8.93×10^4-fold CTX-M-15 up-regulation was needed for the hydrolysis of PIP in the presence of the TAZ to confer the observed levels of PIP-TAZ resistance seen in our STK by this mechanism. This value was more than 100-fold higher than the maximum extent of β-lactamase up-regulation reported in the literature

Table 2 One-population model estimates for the growth and PIP-TAZ pharmacodynamics

Parameters	Value (95% confidence interval)	Units
Natural growth rate[a]	1.43 (1.23–1.67)	h^{-1}
Maximum population size[a]	1.36×10^9 ($8.94 \times 10^8 - 2.08 \times 10^9$)	CFU/mL
Baseline β-lactamase level (R_0)	1.36×10^5 ($1.33 \times 10^5 - 1.39 \times 10^5$)	μM
Inoculum size	8.01×10^5 ($8.00 \times 10^5 - 8.01 \times 10^5$)	CFU/mL
Maximum bactericidal effect (*Emax*)	3.93 (3.92–3.95)	h^{-1}
Intracellular PIP concentration for half-maximum bactericidal effect (EC_{50})	1.44 (1.43–1.44)	μM
Hill exponent of bactericidal effect (H)	3.82 (3.81–3.84)	

[a]parameter value predicted based on observation made in the absence of PIP-TAZ

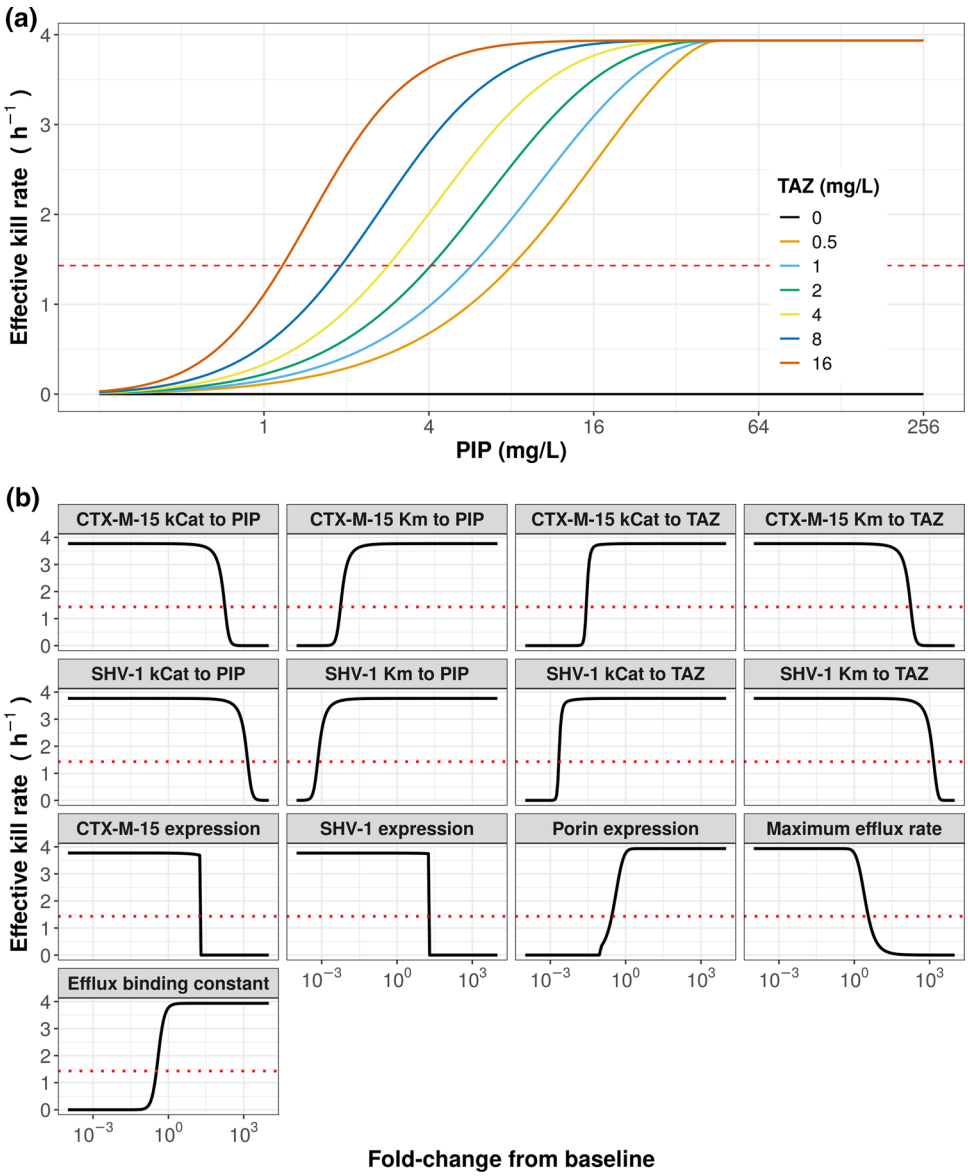

Fig. 2 PIP-TAZ pharmacodynamics on *K. pneumoniae* GR112.6 before the onset of regrowth. The assessment was performed using a one-population model and was based on experimental observations during the first 5 h of the culture. **a** Simulation using the one-population model described how increasing TAZ concentration allowed a higher bactericidal effect to be reached at a lower extracellular PIP concentration. Dashed red line denotes the natural growth rate. **b** The capacity of each resistance mechanism to allow strain survival in 16 – 4 mg/L PIP-TAZ. Dashed red lines represent the natural growth rate

(up to 300-fold up-regulation compared to the expression level of the strain of reference; Table 3), making CTX-M-15 up-regulation an unlikely single-event mechanism mediating the PIP-TAZ resistance observed in our experiment. 3 out of the 13 resistance mechanisms, namely decreased TAZ catalytic rate by SHV-1 and CTX-M-15 β-lactamases as well as increased drug affinity to efflux pumps were excluded due to the lack of experimental evidence of its occurrence in the literature, even though our analysis showed that either of these mechanisms can potentially serve as a single-mechanism mediator to PIP-TAZ resistance by permitting high intracellular TAZ concentrations.

Two of the mechanisms evaluated in this study could promote PIP-TAZ resistance without requiring cellular changes that were more extreme than what was reported in the literature (Table 2; Fig. 3). The first mechanism identified in our workflow was the reduction of PIP-TAZ permeability through the outer membrane, leading to decreased intracellular concentrations of PIP and/or TAZ. A decrease in PIP-TAZ permeability predicted by our model (9.36×10^{-2}-fold decrease compared to the initial susceptible population) can be achieved by down-regulation or loss of porins, the proteins that facilitate PIP-TAZ entry into the periplasm [17, 26]. A previous study supported our model prediction by highlighting the role of OmpK35 porin in facilitating BL transport into *K. pneumoniae* cells and by further revealing the central role of its deletion in the development of BL resistance [32]. The second mechanism highlighted in our workflow was the 21.5-fold increase in efflux pump activity in the resistant population compared to that of the initial susceptible population. Increased efflux pump activity is often mediated by up-regulation of one or more efflux pumps. In

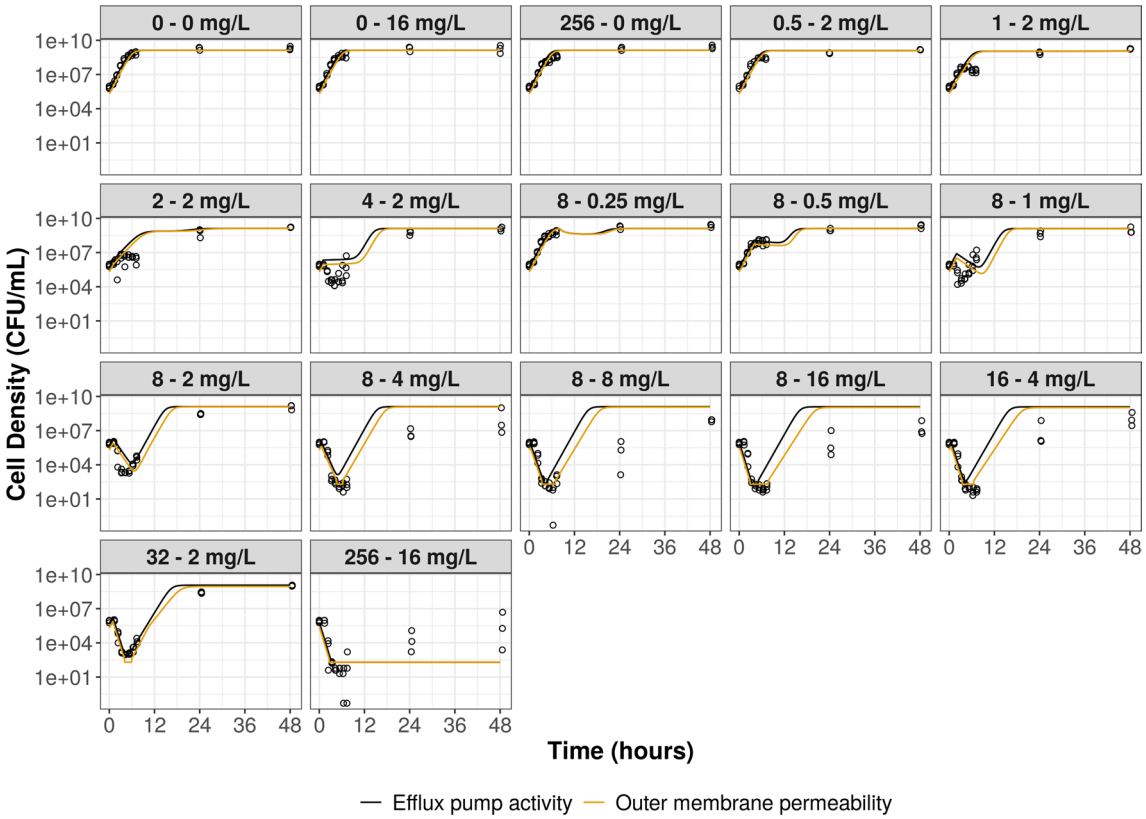

Fig. 3 Population growth prediction using porin down-regulation and efflux pump up-regulation models. Data points represented individual observation obtained during the STK experiment. Lines represented the typical prediction performed using the efflux pump up-regulation model (efflux pump activity) and porin down-regulation model (outer membrane permeability). Drug concentrations were presented in the following format: PIP concentration-TAZ concentration, each in mg/L

K. pneumoniae, the up-regulation of *oqxA*, *kexD*, *kpnF*, and *acrB* efflux pumps were observed in isolates showing different ranges of β-lactam resistance [33]. Overall, the current workflow identified reduction of drug influx and increased efflux pump activity as mechanisms that may independently mediate PIP-TAZ resistance to the level that was observed in our experimental setting.

Both porin down-regulation and efflux pump up-regulation models over-estimated population growth at PIP-TAZ concentrations of 8 − 4, 8–8, 8–16, and 16 − 4 mg/L while under-estimated the regrowth at 256 − 16 mg/L. These deviations could be caused by the application of first-order kinetics used to describe the development of resistance in our models. This implied that our models are constrained to the characterization of resistance as a unimodal process, whereas, in reality, the development of resistance could potentially encompass a complex, multi-stage mechanism. The disagreement between observation and model prediction at these concentration ranges may also be rooted to the use of literature-based parameters that were derived from a different bacterial strain and/or species. To further investigate the issue, a parameter sensitivity analysis was conducted to evaluate the model parameters' influence on the model prediction. The analysis indicated the relatively higher sensitivity of the model estimates towards PIP-TAZ influx and efflux parameters compared to other literature-based parameters used in our models (Fig. S7). While the current parameter sets represented the best available information for the present study, future studies are suggested to characterize these parameters to represent the PIP-TAZ influx and efflux more accurately in the model, thereby improving the predictive capability of the models.

The current study substituted measurement observations below the LLoQ with LLoQ/2. This method of LoQ handling may lead to the overestimation of minimum population size, particularly in instances where the PIP-TAZ bactericidal effect suppressed the bacterial population below the quantifiable limit. Consequently, this approach might introduce additional bias into the estimation of the first-order mutation rate constant ($k_{transfer}$), especially at higher PIP-TAZ concentrations where measurement values fell below the LLoQ. While our sensitivity analysis demonstrates the impact of deviation in $k_{transfer}$ value towards model prediction was found to relatively limited compared to other

Table 3 Fold-change of parameters required to describe the observed level of PIP-TAZ resistance

Affected parameter		Physiological relevance	Magnitude (Fold-change)	Magnitude observed in literatures
Outer membrane permeability	P	·Porin loss ·Reduced porin permeability	9.63×10^{-2}	Down-regulation or complete inactivation of OmpK35/36 [26][a]
Maximum efflux rate	$V_{efflux,\ max}$	·Increased efflux pump expression ·Increased maximum efflux rate	2.15×10^{1}	*oqxB, rarA, acrA, ketM*, *kdeA*, *kpnF*, and *kexD* up-regulation; up to 1.08×10^{3}-fold [27][b]
Efflux pump binding constant	K_{efflux}	Increased PIP-TAZ affinity to efflux pumps	2.00×10^{-2}	No previous report found.
Baseline CTX-M-15 level	$R0_{CTX-M-15}$	Increased baseline β-lactamase level	8.93×10^{4}	β-lactamase up-regulation within 10 to 300-fold [28, 29]
Baseline SHV-1 level	$R0_{SHV-1}$		1.02×10^{4}	
CTX-M-15 PIP catalytic rate	$k_{Cat,\ CTX-M-15,\ PIP}$	Increased PIP hydrolysis rate	2.97×10^{5}	TEM mutants may increase up to 515-fold catalytic rate to a specific compound [30][c]
SHV-1 PIP catalytic rate	$k_{Cat,\ SHV-1,\ PIP}$		7.29×10^{5}	
CTX-M-15 TAZ catalytic rate	$k_{Cat,\ CTX-M-15,\ TAZ}$	Decreased TAZ hydrolysis rate	1.37×10^{-6}	No previous report found
SHV-1 TAZ catalytic rate	$k_{Cat,\ SHV-1,\ TAZ}$		3.05×10^{-6}	
CTX-M-15 PIP Michaelis constant	$Km_{CTX-M-15,\ PIP}$	Increased β-lactamase affinity to PIP	1.61×10^{-2}	Decrease in *Km* values by approximately 0.5-fold in SHV-1 against several β-lactams [31]
SHV-1 PIP Michaelis constant	$Km_{SHV-1,\ PIP}$		8.29×10^{-2}	
CTX-M-15 TAZ Michaelis constant	$Km_{CTX-M-15,\ TAZ}$	Reduced in β-lactamase affinity to TAZ	2.57×10^{3}	Up to 60-fold increase in SHV-1 K_m to TAZ [20]
SHV-1 TAZ Michaelis constant	$Km_{SHV-1,\ TAZ}$		3.63×10^{4}	

[a]May be associated with the up-regulation of other porin subtypes

[b]May be associated with the down-regulation of other efflux pump(s)

[c]Evolutionary tradeoff may lower hydrolysis rate of other β-lactams

literature-derived parameters (Fig. S7), future studies may explore more advanced LoQ handling methods, such as those similar to methods M3 or M4 implemented in NONMEM [34], as potential approaches for handling LoQ in the analysis of STK experiment data.

Exploring the efficiency of PIP-TAZ concertation ranges

The following simulations were performed to explore and evaluate the efficiency of PIP-TAZ concentration ranges beyond its commonly applied 8:1 dosing ratio [4] (Fig. 4, Fig. S8). The simulations were performed using the porin down-regulation and efflux pump up-regulation models, the two key resistance mechanisms identified in the previous step. The expected area of inhibitory PIP-TAZ ranges varied depending on the underlying resistance mechanism. This area of 24-hours growth inhibition was defined as the concentrations in which the growth of the strain was inhibited to a level that population size observed at the 24th hours was less than its size in the beginning of the simulation.

By overlapping the ranges of inhibitory PIP-TAZ concentrations derived from each resistance models, our analysis determined the range of PIP-TAZ concentrations that are expected to suppress the growth of the susceptible as well as the resistant bacterial-subpopulations, irrespective of the underlying resistance mechanism (Fig. 4, double-shaded area). This suggested the possibility to select specific PIP-TAZ doses that impede bacterial growth even if resistance development occurred during treatment. Notably, the range of inhibitory PIP-TAZ concentrations identified in this exercise represents a space of concentrations that is not bound to the widely used 8:1 dose ratio of PIP:TAZ [4]. It may thus be beneficial for future studies to explore and optimize PIP-TAZ doses without the constraint of the currently used 8:1 dose ratio.

Discussion

Understanding the individual impact of different resistance mechanisms offers critical information to identify systems that hold the most potential as pharmacological targets to counter the development of antibiotic resistance [15, 35]. The current study demonstrated how semi-mechanistic models can be used to identify critical PIP-TAZ resistance

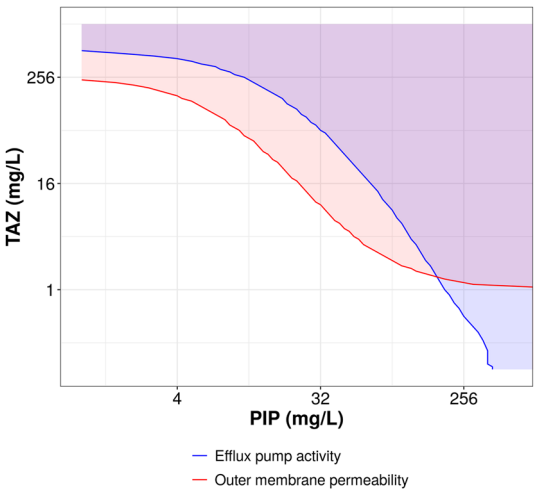

Fig. 4 Predicted PIP-TAZ concentration range to inhibit the growth of CTX-M-15-producing *K. pneumoniae* based on the underlying resistance mechanism. Simulations were performed using the porin down-regulation and efflux pump up-regulation models with an initial population size of 10^5 CFU/mL. Shaded area represents the range of PIP-TAZ concentrations where growth inhibition at 24 h was expected for the specific resistance mechanism

mechanisms based on an STK experiment. Here, several semi-mechanistic models were developed to individually explore the potential involvement of specific mechanisms in reducing periplasmic PIP-TAZ concentration. Our analysis explored the extent in which changes in porin, efflux pump, and β-lactamase expression and functional capability may mediate PIP-TAZ resistance in a CTX-M-15-producing *K. pneumoniae* strain (Fig. 1).

Our analysis identified porin down-regulation as well as efflux pump up-regulation as potential key mediators of PIP-TAZ resistance. Our *in-silico* findings agree with previous experimental studies performed in a similar setting that underlined the importance of porin loss and increase in efflux pump activity in mediating BL-BLI resistance [26, 27]. Unlike changes in β-lactamase activity, changes in porin and efflux pump activities are often seen as a minor concurrence to β-lactamase-related resistance mechanisms [33]. In contrast to this view, our analysis showed that the two resistance mechanisms are individually capable to convey the observed extent of PIP-TAZ resistance. Notably, the regulation of porin [36] and efflux pump [37] expression also play a key role in controlling the osmolarity of a bacterial cell. Regulatory network controlling the expression of porin and efflux pumps are thus present in most – if not all – Gram-negative bacteria [38]. Knowing the important role of osmotic pressure during BL-induced cell lysis [39], it can be hypothesized that the same network of porin and efflux pump regulation, as well as mutational events associated with the network, is triggered when the cell is exposed to PIP-TAZ. Subsequently, this network of porin and efflux pump regulation may provide a path to resistance that is likely to be shared among Gram-negative bacteria.

Although the current study highlighted two single-event mechanisms as key mechanisms to PIP-TAZ resistance, these mechanisms may occur alongside other resistance mechanisms. For example, previous studies revealed how a decrease in outer membrane permeability can coincide with altered β-lactamase activity in a single *K. pneumoniae* strain [40]. These reports hinted the potential value of a model that can simultaneously explore multiple resistance mechanisms, although additional measurement on the specific resistant mechanism might be needed to maintain the certainty of the parameter estimates. Our analysis did not exclude the potential contribution of resistance mechanisms beyond porin loss and efflux pump up-regulation. Previous studies also associated the remaining resistance mechanisms to resistant phenotypes against BL-type antibiotics with or without BLI pairing in bacteremia (Table 3). However, the extent of cellular changes estimated in our models for the remaining 11 resistance mechanisms could not be supported by past experimental observation. This suggested the unlikely role of these mechanisms as a sole driver of PIP-TAZ resistance as observed in our experiment.

Our analysis also utilized porin down-regulation and efflux pump up-regulation models to explore how different these two mechanisms may impact the expected bacterial growth at a higher PIP-TAZ concentration (Fig. 4, Fig. S8). In this context, our models were used as a learning tool to explore the effectivity of PIP-TAZ doses beyond its generally applied 8:1 dosing ratio [4]. Consequently, this opened the possibility for future studies to attempt further optimization of PIP-TAZ doses in anticipation for a specific resistance mechanism while considering the safety limits of PIP-TAZ dosing [41].

Mathematical models represent simplifications of more complex (biological) phenomena. Such simplification can be necessary to describe events that are not well characterized and to derive a more generalized representation of cellular events. Nevertheless, the exclusion of some details may lead to loss of potentially important information. In our models, drug influx through porins were simplified into a single diffusion model despite the presence of multiple porin subtypes in *K. pneumoniae* [26, 32]. This simplification prevented us from identifying a specific porin subtype that may be the most prevalent in conveying resistance to PIP-TAZ. Similarly, the binding of PIP to different PBP variants and its associated bactericidal effect was simplified into an empirical concentration-effect equation (Eq. 7). This prevented us from using the model to explore PBP-related resistance mechanisms. Nevertheless, the empirical simplification of drug effect was necessary due to the limited information on PIP interaction with different PBP variants and the consequence of this interaction on the resulting bactericidal effect.

While a more detailed mechanistic model can be superior in describing a complex biological event, over-extending model complexity, for example by implementing PBP interactions with PIP-TAZ without sufficient data to support such an interaction, may impair the certainty of the resulting parameter estimates [42]. Additional studies to determine the dynamics of these interactions are thus needed to build a more detailed model. Our model also simplified the development of resistant bacterial sub-population using a first-order kinetics (Eqs. 9 and 10). Thus, the development of resistance was depicted as a stepwise event. Consequently, the models were unable to depict neither gradual nor dose-responsive development of resistance. This limitation may, in part, explain the predictive inaccuracies during regrowth events at higher PIP-TAZ concentrations despite the relatively more accurate prediction observed at lower PIP-TAZ concentrations (Fig. 3).

The semi-mechanistic models presented in this study were partly developed using bioanalytical information adopted from other bacterial species and strains. This decision was made due to the unavailability of PIP-TAZ and *K. pneumoniae*-specific parameter values at the time of the study. Considering the potential differences in these system-specific characteristics, the incorporation of PIP-TAZ and *K. pneumoniae*-specific parameters may prove beneficial for future efforts to enhance the descriptive and predictive capabilities of the semi-mechanistic model. Therefore, future studies may focus on investigating these mechanisms to further characterize PIP-TAZ resistance in *K. pneumoniae*.

Conclusion

The current study presents a semi-mechanistic mathematical modeling workflow and its application to complement experimental studies on antimicrobial pharmacodynamics and resistance. Here, we demonstrated the utility of semi-mechanistic models in theoretical exploration highlighting porin down-regulation and efflux pump up-regulation as key mediators of PIP-TAZ resistance. Consequently, our analysis emphasized the importance of these two mechanisms as prospective focal points for future studies aimed at exploring strategies against PIP-TAZ resistance. Moreover, we illustrated how the resulting models can be used to evaluate the effectivity of PIP-TAZ concentration ranges in suppressing bacterial growth during the emergence of a specific resistance mechanism. In conclusion, our study demonstrated the utility of semi-mechanistic models in complementing experimental efforts to provide insight into the relative impact of potential resistance mechanisms on antibiotic treatment response, help guide subsequent experimental designs, and support the rational design of antibiotic treatment to against resistance development.

Supplementary Information The online version contains supplementary material available at https://doi.org/10.1007/s10928-023-09895-3.

Author contributions ST, LA, and CH conceived the presented idea. ST and EL collected experimental results and explored different analytical angles. AL counseled the details of the strain's resistance mechanism implementation on the model. CH supervised and evaluated the work. ST wrote the main manuscript text. All authors reviewed the manuscript.

Funding The authors did not receive any funding for this work.

Declarations

Competing interests The authors declare no competing interests.

References

1. Oliphant CM, Eroschenko K (2015) Antibiotic resistance, Part 2: gram-negative pathogens. JNP-J Nurse Pract 11:79–86
2. Dhillon RH, Clark J (2012) ESBLs: a clear and present danger? Crit Care Res Pract 2012:625170
3. Drawz SM, Bonomo RA (2010) Three decades of beta-lactamase inhibitors. Clin Microbiol Rev 23(1):160–201. https://doi.org/10.1128/CMR.00037-09
4. Abodakpi H, Chang KT, Gao S, Sánchez-Díaz AM, Cantón R, Tam VH (2019) Optimal piperacillin-tazobactam dosing strategies against extended-Spectrum-β-Lactamase-producing *Enterobacteriaceae*. Antimicrob Agents Chemother 63(2):e01906–e01918. https://doi.org/10.1128/AAC.01906-18
5. Abdelraouf K, Chavda KD, Satlin MJ, Jenkins SG, Kreiswirth BN, Nicolau DP (2020) Piperacillin-tazobactam-resistant/third-generation cephalosporin-susceptible *Escherichia coli* and *Klebsiella pneumoniae* isolates: resistance mechanisms and in vitro-in vivo discordance. Int J Antimicrob Agents 55(3):105885
6. Zhou K, Tao Y, Han L, Ni Y, Sun J (2019) Piperacillin-Tazobactam (TZP) resistance in Escherichia coli due to hyperproduction of TEM-1 β-Lactamase mediated by the promoter Pa/Pb. Front Microbiol 10:833. https://doi.org/10.3389/fmicb.2019.00833
7. Nicolas-Chanoine MH, Mayer N, Guyot K, Dumont E, Pagès JM (2018) Interplay between membrane permeability and enzymatic barrier leads to antibiotic-dependent resistance in *Klebsiella Pneumoniae*. Front Microbiol 9:1422. https://doi.org/10.3389/fmicb.2018.01422
8. Fernández L, Hancock RE (2012) Adaptive and mutational resistance: role of porins and efflux pumps in drug resistance. Clin Microbiol Rev 25(4):661–681. https://doi.org/10.1128/CMR.00043-12
9. Pages JM, Lavigne JP, Leflon-Guibout V, Marcon E, Bert F, Noussair L, Nicolas-Chanoine MH (2009) Efflux pump, the masked side of beta-lactam resistance in *Klebsiella pneumoniae* clinical isolates. PLoS ONE 4(3):e4817. https://doi.org/10.1371/journal.pone.0004817
10. Kakoullis L, Papachristodoulou E, Chra P, Panos G (2021) Mechanisms of antibiotic resistance in important gram-positive and gram-negative pathogens and novel antibiotic solutions. Antibiot (Basel Switzerland) 10(4):415. https://doi.org/10.3390/antibiotics10040415
11. Heinz E, Ejaz H, Bartholdson Scott J, Wang N, Gujaran S, Pickard D, Wilksch J, Cao H, Haq IU, Dougan G, Strugnell

RA (2019) Resistance mechanisms and population structure of highly drug resistant Klebsiella in Pakistan during the introduction of the carbapenemase NDM-1. Sci Rep 9(1):2392. https://doi.org/10.1038/s41598-019-38943-7
12. Masi M, Réfregiers M, Pos KM, Pagès JM (2017) Mechanisms of envelope permeability and antibiotic influx and efflux in gram-negative bacteria. Nat Microbiol 2:17001. https://doi.org/10.1038/nmicrobiol.2017.1
13. Prochnow H, Fetz V, Hotop SK, García-Rivera MA, Heumann A, Brönstrup M (2019) Subcellular quantification of uptake in gram-negative bacteria. Anal Chem 91(3):1863–1872. https://doi.org/10.1021/acs.analchem.8b03586
14. Mi K, Zhou K, Sun L, Hou Y, Ma W, Xu X, Huo M, Liu Z, Huang L (2022) Application of semi-mechanistic pharmacokinetic and pharmacodynamic model in antimicrobial resistance. Pharmaceutics 14(2):246. https://doi.org/10.3390/pharmaceutics14020246
15. Sahoo S, Mishra A, Kaur H, Hari K, Muralidharan S, Mandal S, Jolly MK (2021) A mechanistic model captures the emergence and implications of non-genetic heterogeneity and reversible drug resistance in ER + Breast cancer cells. NAR cancer 3(3):zcab027. https://doi.org/10.1093/narcan/zcab027
16. Liakopoulos A, Betts J, La Ragione R, van Essen-Zandbergen A, Ceccarelli D, Petinaki E, Koutinas CK, Mevius DJ (2018) Occurrence and characterization of extended-spectrum cephalosporin-resistant enterobacteriaceae in healthy household dogs in Greece. J. Med. Microbiol 67(7):931–935
17. Kojima S, Nikaido H (2013) Permeation rates of penicillins indicate that *Escherichia coli* porins function principally as nonspecific channels. PNAS 110(28):E2629–E2634
18. Lim SP, Nikaido H (2010) Kinetic parameters of efflux of penicillins by the multidrug efflux transporter AcrAB-TolC of *Escherichia coli*. Antimicrob Agents Chemother 54(5):1800–1806. https://doi.org/10.1128/AAC.01714-09
19. Faheem M, Rehman MT, Danishuddin M, Khan AU (2013) Biochemical characterization of CTX-M-15 from Enterobacter cloacae and designing a novel non-β-lactam-β-lactamase inhibitor. PLoS ONE 8(2):e56926. https://doi.org/10.1371/journal.pone.0056926
20. Helfand MS, Bethel CR, Hujer AM, Hujer KM, Anderson VE, Bonomo RA (2003) Understanding resistance to beta-lactams and beta-lactamase inhibitors in the SHV beta-lactamase: lessons from the mutagenesis of SER-130. J Biol Chem 278(52):52724–52729. https://doi.org/10.1074/jbc.M306059200
21. Maurizi MR (1992) Proteases and protein degradation in *Escherichia coli*. Experientia 48(2):178–201. https://doi.org/10.1007/BF01923511
22. Perilli M, Franceschini N, Bonfiglio G, Segatore B, Stefani S, Nicoletti G, Perez MM, Bianchi C, Zollo A, Amicosante G (2000) A kinetic study on the interaction between tazobactam (a penicillanic acid sulphone derivative) and active-site serine beta-lactamases. J Enzyme Inhib 15(1):1–10. https://doi.org/10.1080/14756369909030337
23. Nielsen EI, Friberg LE (2013) Pharmacokinetic-pharmacodynamic modeling of antibacterial drugs. Pharmacol Rev 65(3):1053–1090. https://doi.org/10.1124/pr.111.005769
24. Viane E, Chanteux H, Servais H, Mingeot-Leclercq M-P, Tulkens PM (2002) Comparative Stability Studies of antipseudomonal-lactams for potential administration through portable elastomeric pumps (home therapy for cystic fibrosis patients) and motor-operated syringes (intensive care units). Antimicrob Agents Chemoter 46(8):2327–2332. https://doi.org/10.1128/AAC.46.8.2327-2332.2002
25. Samara E, Moriarty TF, Decosterd LA, Richards RG, Gautier E, Wahl P (2017) Antibiotic stability over six weeks in aqueous solution at body temperature with and without heat treatment that mimics the curing of bone cement. Bone Jt Res 6(5):296–306. https://doi.org/10.1302/2046-3758.65.BJR-2017-0276.R1
26. Kaczmarek FM, Dib-Hajj F, Shang W, Gootz TD (2006) High-level carbapenem resistance in a *Klebsiella pneumoniae* clinical isolate is due to the combination of bla(ACT-1) beta-lactamase production, porin OmpK35/36 insertional inactivation, and down-regulation of the phosphate transport porin phoe. Antimicrob Agents Chemother 50(10):3396–3406. https://doi.org/10.1128/AAC.00285-06
27. Lee YJ, Huang CH, Ilsan NA, Lee IH, Huang TW (2021) Molecular epidemiology and characterization of carbapenem-resistant *Klebsiella pneumoniae* isolated from urine at a teaching hospital in Taiwan. Microorganisms 9(2):271. https://doi.org/10.3390/microorganisms9020271
28. Singh T, Singh PK, Das S, Wani S, Jawed A, Dar SA (2019) Transcriptome analysis of beta-lactamase genes in diarrheagenic *Escherichia coli*. Sci Rep 9(1):3626. https://doi.org/10.1038/s41598-019-40279-1
29. Jones AK, Ranjitkar S, Lopez S, Li C, Blais J, Reck F, Dean CR (2018) Impact of Inducible blaDHA-1 on susceptibility of Klebsiella pneumoniae clinical isolates to LYS228 and identification of chromosomal mpl and ampD mutations mediating Upregulation of plasmid-borne blaDHA-1 expression. Antimicrob Agents Chemother 62(10):e01202–e01218. https://doi.org/10.1128/AAC.01202-18
30. Wang X, Minasov G, Shoichet BK (2002) Evolution of an antibiotic resistance enzyme constrained by stability and activity trade-offs. J Mol Biol 320(1):85–95. https://doi.org/10.1016/S0022-2836(02)00400-X
31. Ramdani-Bouguessa N, Manageiro V, Jones-Dias D, Ferreira E, Tazir M, Caniça M (2011) Role of SHV β-lactamase variants in resistance of clinical *Klebsiella pneumoniae* strains to β-lactams in an Algerian hospital. J Med Microbiol 60(Pt 7):983–987. https://doi.org/10.1099/jmm.0.030577-0
32. Tsai YK, Fung CP, Lin JC, Chen JH, Chang FY, Chen TL, Siu LK (2011) *Klebsiella pneumoniae* outer membrane porins OmpK35 and OmpK36 play roles in both antimicrobial resistance and virulence. Antimicrob Agents Chemother 55(4):1485–1493. https://doi.org/10.1128/AAC.01275-10
33. Maurya N, Jangra M, Tambat R, Nandanwar H (2019) Alliance of efflux pumps with β-lactamases in multidrug-resistant *Klebsiella pneumoniae* isolates. Microb Drug Resist 25(8):1155–1163. https://doi.org/10.1089/mdr.2018.0414
34. Bergstrand M, Karlsson MO (2009) Handling data below the limit of quantification in mixed effect models. AAPS J 11(2):371–380. https://doi.org/10.1208/s12248-009-9112-5
35. Clegg LE, Mac Gabhann F (2015) Molecular mechanism matters: benefits of mechanistic computational models for drug development. Pharmacol Res 99:149–154. https://doi.org/10.1016/j.phrs.2015.06.002
36. Graeme-Cook KA (1991) The regulation of porin expression in *Escherichia coli*: effect of turgor stress. FEMS Microbiol Lett 63(2–3):219–223. https://doi.org/10.1016/0378-1097(91)90089-s
37. Zhu M, Dai X (2018) High salt cross-protects *Escherichia coli* from antibiotic treatment through increasing efflux pump expression. mSphere 3(2):e00095–e00018. https://doi.org/10.1128/mSphere.00095-18
38. Ferrand A, Vergalli J, Pagès JM, Davin-Regli A (2020) An intertwined network of regulation controls membrane permeability including drug influx and efflux in enterobacteriaceae. Microorganisms 8(6):833. https://doi.org/10.3390/microorganisms8060833
39. Wong F, Wilson S, Helbig R, Hegde S, Aftenieva O, Zheng H, Liu C, Pilizota T, Garner EC, Amir A, Renner LD (2021) Understanding beta-lactam-induced lysis at the single-cell level. Front Microbiol 12:712007. https://doi.org/10.3389/fmicb.2021.712007

40. Khalifa SM, El-Aziz A, Hassan AM, Abdelmegeed ES (2021) β-lactam resistance associated with β-lactamase production and porin alteration in clinical isolates of *E. coli* and *K. pneumoniae*. PLoS ONE 16(5):e0251594. https://doi.org/10.1371/journal.pone.0251594
41. Kim MK, Xuan D, Quintiliani R, Nightingale CH, Nicolau DP (2001) Pharmacokinetic and pharmacodynamic profile of high dose extended interval piperacillin-tazobactam. J Antimicrob Chemother 48(2):259–267. https://doi.org/10.1093/jac/48.2.259
42. Sher A, Niederer SA, Mirams GR, Kirpichnikova A, Allen R, Pathmanathan P, Gavaghan DJ, van der Graaf PH, Noble D (2022) A quantitative systems pharmacology perspective on the importance of parameter identifiability. Bull Math Biol 84(3):39. https://doi.org/10.1007/s11538-021-00982-5